A new ground-based, hourly global lightning climatology

Katrina S. Virts[1], John M. Wallace[1], Michael L. Hutchins[2], and Robert H. Holzworth[2]

[1]Department of Atmospheric Sciences, University of Washington, Seattle, Washington, USA

[2]Department of Earth and Space Sciences, University of Washington, Seattle, Washington, USA

Submitted on 15 June 2012, re-submitted on _____

Corresponding author address: Katrina Virts, Department of Atmospheric Sciences, 408 ATG Bldg., Box 351640, Seattle, WA 98195-1640
Email: kvirts@uw.edu

Abstract

The seasonally and diurnally-varying frequency of lightning flashes provides a measure of the frequency of occurrence of intense convection and, as such, is useful in describing the Earth's climate. Here we present a few highlights of a global lightning climatology based on data from the ground-based World Wide Lightning Location Network (WWLLN), for which global observations began in 2004. Because WWLLN monitors global lightning continuously, it samples ~100 times as many lightning strokes per year as the Tropical Rainfall Measuring Mission's (TRMM) Lightning Imaging Sensor (LIS). Using WWLLN data it is possible to generate a global lightning climatology that captures seasonal variations, including those associated with the mid-latitude storm tracks, and resolves the diurnal cycle, thereby illuminating the interplay between sea breezes, mountain-valley wind systems, and remotely forced gravity waves in touching off thunderstorms in a wide variety of geographical settings. The text of the paper shows a few samples of WWLLN-based regional seasonal (the mid-latitude storm tracks and the Mediterranean) and diurnal climatologies (the Maritime Continent, the central Andes, and equatorial Africa), and the on-line supplement presents animations of the global seasonal cycle and of the diurnal cycle for the latter regions.

Capsule

The ground-based World Wide Lightning Location Network (WWLLN) provides unprecedented sampling of lightning frequency, providing a basis for climatologies that resolve diurnal as well as seasonal variations.

1. Introduction

Much of the rain that falls in the tropics is associated with deep cumulus convection (Lopez 1978; Rickenbach and Rutledge 1998; Johnson et al 1999). The clouds exhibit a characteristic life cycle with newly-formed, buoyant convective cells consisting of air that has been lifted to its level of free convection in the lower troposphere and begins to ascend freely (Ogura and Takahashi 1971; Houze 1993, chapter 7), drawing on the convective available potential energy (CAPE) inherent in the conditionally unstable mid-troposphere (Williams and Renno 1993). Within an hour or so, the growing cells encounter the stably stratified tropical tropopause transition layer ~12 km (Highwood and Hoskins 1998; Gettelman and Forster 2002), whereupon they spread out to form much longer lived "anvils" in which the air continues to rise, but much more slowly (Yuan et al. 2011). Over the tropics as a whole, roughly half the rain falls as heavy, but short-lived showers from the updrafts in convective cells, and the other half falls more gently in mesoscale rain areas formed by spreading anvil clouds (Schumacher and Houze 2003). Convective cells originating over the oceans tend to be of moderate intensity with updraft speeds on the order of 1-2 m s^{-1}, whereas those originating over land when the buoyancy of boundary layer air is enhanced by daytime heating may have updraft velocities up to 5 m s^{-1} or more (Stith et al. 2002), which is strong enough to induce the rates of charge separation required to produce lightning (Deierling and Petersen 2008). Hence, the frequency of occurrence of lightning serves as a proxy for the frequency of occurrence of vigorous updrafts and associated phenomena such as flash floods (Tapia et al. 1998).

Conditionally unstable lapse rates in the mid-troposphere are a necessary condition for vigorous convection, but in order to realize the CAPE inherent in the temperature stratification it is necessary to have sufficient low level convergence to lift stably stratified boundary layer air up

to its level of free convection (Williams and Renno 1993). In the tropics, where synoptic scale disturbances are generally weak, land-sea breezes and mountain-valley wind regimes forced by the diurnal cycle in low level heating are the dominant mechanism for producing the required lifting (Kikuchi and Wang 2008). Daytime heating of the boundary layer air over land can greatly increase the CAPE that can be realized if there is sufficient lifting to trigger convection. It follows that lightning frequency should be strongly modulated by the diurnal cycle and, indeed, it has been shown to be so in numerous regional studies in different parts of the world (among others, Petersen et al. 1996; Pinto et al. 1999; Collier et al. 2006).

In contrast with the predominantly locally-driven thunderstorms in the tropics, thunderstorms (Pessi and Businger 2009) and heavy precipitation (Jansa et al. 2001) in the extratropics are known to occur in association with synoptic scale cyclones. During winter, cyclones tend to form in the lee of mountain ranges, such as the Andes (Hoskins and Hodges 2005) and Rockies (Zishka and Smith 1980; Schultz and Doswell 2000), and over the western oceanic boundary currents and propagate eastward across the oceans, forming so-called "storm tracks" of enhanced cyclone activity (Hoskins and Valdes 1990; Hoskins and Hodges 2005). Wintertime cyclones are also observed over the Mediterranean Sea (Karas and Zangvil 1999).

Until recently, lightning climatologies have been based on station data or local lightning networks, most of which are regional or national in scope. Global satellite-based lightning monitoring began in the 1970s (Turman 1978, and references therein; Orville and Spencer 1979), and statistically significant lightning climatologies became available with the development of the Optical Transient Detector (OTD) and the Lightning Imaging Sensor (LIS; Christian et al. 2000). Datasets derived from these measurements have been used to construct annual-mean and

91 seasonal lightning climatologies (Christian et al. 1999, 2003) and to investigate tropical-mean
92 diurnal lightning variability (Liu and Zipser 2008).

93 The World Wide Lightning Location Network (WWLLN, see http://wwlln.net) is a
94 ground-based network with global observations beginning in 2004. The WWLLN record is now
95 long enough to support studies of seasonal, diurnal, and synoptic lightning variability over most
96 of the globe. Descriptions of the WWLLN and LIS datasets are in Section 2, and a comparison
97 of the climatological distribution of lightning detected by each sensor is in Section 3. Seasonal
98 and diurnal variations in lightning frequency observed by WWLLN are discussed in Section 4,
99 followed by conclusions in Section 5.
100

101 **2. Data**

102 The WWLLN network consists of 68 sensors, as of October 2012 (sensor locations are
103 shown in Fig. 1), that monitor very low frequency (VLF) radio waves for lightning sferics. The
104 network uses a time of group arrival technique (Dowden et al. 2002) on the detected sferic
105 waveforms to locate lightning to within ~5 km and < 10 μs (Abarca et al. 2010). Comparisons
106 between lightning observations from WWLLN and regional networks indicate that the global
107 detection efficiency of WWLLN can be estimated as ~10% (Rodger et al. 2006, 2009; Abarca et
108 al. 2010; Connaughton et al. 2010; Hutchins et al. 2012b) of all strokes, which is sufficient to
109 enable WWLLN to detect almost all lightning-producing storms (Jacobson et al. 2006).

110 Abarca et al. (2010) compared WWLLN hourly lightning frequency over the United
111 States with observations from the National Lightning Detection Network (NLDN) and found
112 some marked differences. The agreement was somewhat better when comparing subsets of each
113 climatology corresponding to strokes with strong peak currents, but the dfferences were still

large enough that they expressed reservations concerning the ability of WWLLN to capture the diurnal cycle. We will show in Section 4 that the WWLLN hourly climatology is generally consistent with prior ground-based studies and with our understanding of the processes that cause lightning to vary systematically with time of day.

OTD was launched with the MicroLab-1 satellite in April 1995 into a 70° inclination orbit (Christian et al. 2003), and LIS is carried on the Tropical Rainfall Measuring Mission (TRMM) satellite, which was launched in 1997 into a 35° inclination orbit (Christian et al. 1999). In this study, we make use of lightning climatologies based on ~13 years of LIS and ~5 years of OTD observations. Annual-mean and hourly-mean climatologies are available at 0.5° and 2.5° spatial resolution, respectively. TRMM also carries a Precipitation Radar (PR) and Visible and Infrared Scanner (VIRS). TRMM rainfall observations are supplemented with data from other satellite-borne microwave imagers and infrared sensors to generate the gridded TRMM 3B42 dataset (Huffman et al. 2007), which is available at 3-hourly temporal resolution and 0.25° spatial resolution.

Given the complexity of lightning, understanding the differences between lightning climatologies based on observations from different instruments or networks is a work in progress. LIS/OTD and WWLLN rely on fundamentally different detection methods. WWLLN receivers detect sferics which have propagated in the Earth-ionosphere waveguide and are fully captured within a 1 millisecond window at each station (Dowden et al. 2002). Because WWLLN has a relatively high detection threshold for power, it preferentially detects strong cloud to ground strokes and rarely detects and locates multiple strokes within a single flash (Rodger et al. 2004, 2005; Jacobson et al. 2006). Thus, strictly speaking, WWLLN detects lightning strokes, not lightning flashes. In contrast, LIS and OTD are optical staring imagers that detect

momentary changes in cloud brightness caused by lightning. Optical transients that are similarly located in space and time are grouped into events referred to as flashes (Christian et al. 2000). Thus, we will compare climatologies of WWLLN strokes with climatologies of LIS/OTD flashes, while acknowledging the differences in the type of lightning detected by each instrument. Further specifics on WWLLN may be found in Section 1 of the supplementary material and in the peer-reviewed articles listed at http://wwlln.net/publications.

3. TRMM LIS versus WWLLN annual-mean lightning climatologies

The frequency of occurrence of lightning, as detected by WWLLN during the years 2008-2011, is compared with LIS/OTD observations in Figs. 2*a*, *b*. The two climatologies are qualitatively similar, both showing a concentration of lightning over major tropical continents—Africa, southeastern Asia and Australasia, and Central and South America—with strong gradients near the coastlines and features that bear a strong relationship to the underlying topography (Fig. S2). For example, lightning is frequently observed in the central United States between the Rocky and Appalachian Mountains. Both lightning climatologies differ substantially from the TRMM rainfall climatology shown in Fig. 3*a*, in which the maxima are over the oceanic "warm pool" covering the equatorial Indian and western Pacific Oceans and in the region of the intertropical convergence zone (ITCZ). Lightning also tends to be more geographically focused than rainfall: in the WWLLN and LIS climatologies for the tropical belt (30°N-30°S), half the lightning strokes are observed in 8% of the area, whereas half the rain falls over 22% of the area (Fig. S3). These distinctions illustrate the importance of daytime heating of the atmospheric boundary layer over land in creating the conditions required for the initiation of intense convection.

The color bars in Figs. 2*a*, *b* have been chosen so as to emphasize the similarities between the LIS/OTD and WWLLN lightning climatologies. Differences between the two climatologies are illustrated in Fig. 2*c*, which shows the point-wise ratio of lightning frequency reported by LIS/OTD and WWLLN. This ratio was then multiplied by a scaling factor—the global mean WWLLN lightning frequency divided by the global mean LIS/OTD lightning frequency—so that values < 1 indicate proportionally more WWLLN lightning, and vice versa, relative to their respective global means. With a few notable exceptions (e.g., over the Maritime Continent and the southeastern United States), LIS/OTD reports proportionally more lightning over land and less over the oceans than WWLLN. Because WWLLN's detection efficiency is higher for lightning strokes with higher peak currents (Rodger et al. 2009), the land/sea contrasts in Fig. 2*c* may reflect a tendency for more powerful lightning strokes over the oceans than over land (Boccippio et al. 2000; Rudlosky and Fuelberg 2010). The unevenness of the spacing of the WWLLN stations (Fig. 1) also contributes to the observed differences between the LIS/OTD and WWLLN climatologies. For example, it is evident from Fig. 2*c* that the LIS lightning climatology places relatively greater emphasis on the maxima in lightning frequency in areas such as Africa and the Himalayas, where WWLLN's detection efficiency is lower (Hutchins et al. 2012b). Further analysis of lightning stroke energy, particularly over the eastern United States, is ongoing.

For broad regional comparisons between lightning frequency over different continental regions, such as central America versus India, LIS is clearly the definitive dataset for latitudes up to ~35°. The advantage of WWLLN is that it samples continuously over the whole globe, whereas LIS and OTD sample only when the satellite passes overhead, or ~0.1% of the time (Christian et al. 1999, 2003). When detection efficiency (~10% for WWLLN [Rodger et al.

2009; Abarca et al. 2010] and ~80-90% for LIS [Boccippio et al. 2002]) is taken into account, WWLLN samples ~100 times as many strokes per year as LIS. The difference in the number of samples has little effect on the appearance of the annual-mean lightning climatologies shown in Fig. 2, but it becomes a more important consideration when the data are broken down by synoptic situation and/or by time of day.

In Section 4 we describe some regional, WWLLN-based seasonal and diurnal lightning climatologies that reveal, with an unprecedented level of detail, how the occurrence of vigorous convection is maximized in the wintertime storm tracks and in the tropics where it is shaped by the underlying topography and land-sea distribution. The diurnal images shown in the text are complemented by 24-hour animations of the climatological-mean diurnal cycle in the online supplement for this article, and a more extensive selection of animations on the WWLLN web site.

4. Seasonal and diurnal characteristics

WWLLN lightning and TRMM precipitation over the northern Pacific and Atlantic Oceans during Northern Hemisphere winter are shown in Fig. 4*a*, *b* and in Fig. 3*b*, *c*, respectively; corresponding maps for the southern Atlantic and Indian Oceans during Southern Hemisphere winter are shown in Fig. 4*c*, *d* and Fig. 3*d*, *e*. The zonally elongated precipitation bands observed in each ocean basin including the South Pacific (not shown) between ~30° and ~50° latitude are associated with the wintertime storm tracks (Huffman et al. 1997); the North Atlantic storm track appears to veer poleward around 45° W. Vigorous convection is also found in the storm tracks, as evidenced by the corresponding lightning bands in Fig. 4. The lightning maxima lie along, or a few degrees equatorward of, the axes of maximum rainfall, and secondary

206 east-west oriented lightning maxima are visible in the North Pacific and Atlantic. Based on data
207 from LIS and the Pacific Lightning Detection Network, Pessi and Businger (2009) concluded
208 that much of the lightning in the storm tracks occurs in thunderstorms embedded in the cold
209 fronts of mid-latitude cyclones. During winter, both lightning densities and rainfall rates are
210 larger over the oceans than over land. Strong gradients are observed along the coasts and over
211 warm western boundary currents. Over Argentina, wintertime cyclone development takes place
212 in the lee of the Andes (Hoskins and Hodges 2005), and the lightning and precipitation maxima
213 both begin over Argentina. Global, monthly-mean lightning animations based on WWLLN and
214 LIS/OTD observations are in the supplementary material.

215 Cyclonic disturbances also produce thunderstorms over the Mediterranean during the
216 local winter season (Defer 2005). Both lightning and precipitation are more frequent over the
217 warmer sea than over the colder European landmass (Fig. 5*a*, *b*), in agreement with previous
218 studies based on data from local lightning networks (Altaratz et al. 2003; Katsanos et al. 2007).
219 Lightning gradients along the northern and eastern coasts of the Mediterranean and Adriatic are
220 particularly sharp where there is steep terrain near the coast. Composite analysis (not shown)
221 shows that southwesterly flow is observed during days of frequent lightning along the
222 northeastern Adriatic coast. In addition, the low level instability produced by colder air moving
223 over the warmer Mediterranean waters can create a favorable environment for thunderstorm
224 development in the absence of cyclones (Altaratz et al. 2003). In contrast, during Northern
225 Hemisphere summer, lightning and precipitation are most frequent over the warmer European
226 continent (Fig. 5*c*, *d*; Chronis 2012), where thunderstorms form over the Alps, the Pyrenees, and
227 the mountains of the Balkan Peninsula. Lightning occurrence over the latter region was also
228 examined by Kotroni and Lagouvardos (2008) using an experimental lightning network.

229 The diurnal cycle of lightning over the Maritime Continent, the central Andes, and the
230 African Great Lakes is summarized in Fig. 6-8 in terms of maps of the climatological frequency
231 of occurrence of lightning during selected segments of the day. These summary maps and the
232 animations in the supplementary material reveal the following characteristics of the diurnal
233 variability.

234 • In response to the diurnal cycle in incoming solar radiation, convection begins around
235 local noon over inland regions with relatively flat terrain such as the Amazon basin (Fig.
236 7) and parts of central Africa (Fig. 8). Over these regions, lightning occurs most
237 frequently during afternoon and early evening, with a late afternoon peak, and least
238 frequently during the morning, despite the fact that attenuation of the VLF waves used by
239 WWLLN to locate lightning strokes is strongest during daytime (Hutchins et al. 2012a).
240 Rainfall over the tropical continents exhibits a diurnal cycle with a similarly-timed peak
241 (Kikuchi and Wang 2008). Diurnal lightning variability is smaller in Argentina (Fig. 7),
242 where long-lived mesoscale convective systems (MCSs; Salio et al. 2007) produce
243 nighttime lightning.

244 • During sunny days, warm air rises along mountain slopes as an anabatic wind, or "valley
245 breeze." Thunderstorms form over the steep terrain just west of the crest of the Andes
246 during late morning and shift to the east of the crest by ~1600 LT, where they linger into
247 early evening. The influence of valley breezes is also evident in the intense
248 thunderstorms that begin in the early afternoon along the western slopes of the Mitumba
249 and Virunga Mountains of central Africa and produce maximum lightning ~1900 LT
250 (Fig. 8; Jackson et al. 2009). Similarly, afternoon and early evening lightning is
251 frequently observed over the slopes of the mountains of the Maritime Continent (Fig. 6).

- At night, cooling air drains down from the mountains into the valleys as a katabatic wind, or "mountain breeze," inducing weak ascent over the lower terrain that is augmented where valleys of adjacent tributaries converge. Lightning occurs on the valley floor to the east of the Andes (Fig. 7), where nocturnal convection tends to be organized into mesoscale convective complexes (Bendix et al. 2009), but not to the west, where the boundary layer air is much drier. Adjacent to the Andes, lightning is observed most frequently just before midnight and persists into the morning of the next day. In some cases, nighttime lightning frequencies are similar in magnitude to the daytime maxima over the mountain slopes. Over the Maritime Continent, the mountains are free of lightning at night, while thunderstorms linger over the surrounding lowlands (Fig. 6).
- Strong diurnal variations in lightning occurrence are also observed near coastlines. On sunny mornings, land surfaces, with their smaller heat capacities, warm up rapidly, resulting in strong temperature and pressure contrasts along coastlines that drive onshore winds, or "sea breezes." Over the Maritime Continent, convection begins around noon as the sea breeze fronts develop and intensify as they propagate inland during the afternoon, with peak lightning frequencies around 1600-1700 LT (Fig. 6). Locally, lightning is enhanced where convex coastlines result in sea breeze convergence; e.g., over parts of Borneo. Most small islands experience brief afternoon lightning maxima ~3-5 hours in duration and become lightning-free by early evening, while thunderstorms over larger islands persist into the evening. Similar behavior has been noted in precipitation duration (Qian 2008). Where mountains and coastlines are in close proximity, sea breezes and valley breezes can act in concert to produce strong afternoon and evening convection (Mahrer and Pielke 1977).

- At night, when the boundary layer over land cools, coastal circulation patterns reverse, resulting in "land breezes." Thunderstorms begin ~2000 LT over Lakes Malawi and Kivu in central Africa and an hour or two later over Lakes Victoria, Tanganyika, and Albert (Fig. 8). Land breezes, enhanced by katabatic winds from the surrounding terrain (Savijärvi and Järvenoja 2000), strengthen and converge over the lakes through the night, and lightning is observed most frequently at ~0400-0500 LT. Over Lake Victoria the lightning maximum shifts from the northeastern part of the lake to the southwestern part by morning; similar behavior was observed by Hirose et al. (2008) based on TRMM precipitation data. No corresponding shift is observed over the other lakes.

Near the Maritime Continent, the nocturnal convection regime is more complex. Locally, land breezes and mountain breezes result in offshore winds, and areas with concave coastlines exhibit enhanced nighttime lightning (Fig. 6). In addition, features in the animations (found in the supplement and at http://wwlln.net/climate) that resemble gravity waves propagate out of the regions of afternoon convection and appear to trigger thunderstorms over the coastal waters, as in the numerical simulations of Mapes et al. (2003). The daytime lightning over the western slopes of the mountains of Sumatra moves offshore in late afternoon into a region of weakening convective inhibition (Wu et al. 2009), propagates southwestward, and weakens after sunrise the following day, in agreement with the description of Mori et al. (2004), based on TRMM rainfall data. Strong convection and frequent lightning occur between 2200 and 1200 LT in the Strait of Malacca, where land breezes from Sumatra and the Malay Peninsula converge (Fujita et al. 2010). Elsewhere, such as along the northern coast of New Guinea, a separate line of thunderstorms forms along the coast just before midnight and moves offshore in the

298 early morning hours. By morning, each of the major islands is surrounded by a ring of
299 lightning, consistent with the TRMM rainfall climatology of Kikuchi and Wang (2008).
300 Diurnal lightning maps for the Maritime Continent based on the LIS/OTD climatology
301 are shown in Fig. 6. The WWLLN and LIS/OTD climatologies are similar in some respects—
302 for example, both indicate that lightning is more frequent over the major islands during the
303 afternoon and evening than during the morning. However, the spatial resolution of the LIS/OTD
304 climatology is too coarse to fully resolve features such as the morning lightning maximum in the
305 Strait of Malacca. Hour-by-hour time series of WWLLN lightning for three areas of interest are
306 in the supplementary material.
307 The discussion in this paper has focused on diurnal lightning variability in the
308 climatological-mean or, for the Andes, the extended local summer season. Phenomena such as
309 the monsoons (Kandalgaonkar et al. 2003), El Niño-Southern Oscillation (Hamid et al. 2001),
310 and the Madden-Julian Oscillation (Kodama et al. 2006) also modulate lightning occurrence and,
311 likely, its diurnal cycle.
312

313 **5. Conclusions**

314 TRMM LIS and WWLLN are the only existing lightning datasets that provide global
315 coverage. LIS provides a well-calibrated tropical lightning climatology that already extends for
316 over 14 years. WWLLN has been in operation for only a few years, but it offers the possibility
317 of monitoring lightning frequency over the entire globe with sample sizes two orders of
318 magnitude larger than is feasible with LIS, as evidenced by the comparison in Fig. 6. The two
319 datasets are highly complementary. The Geostationary Operational Environmental Satellite R-
320 Series (GOES-R) satellite, scheduled for launch in 2015, will carry aboard a lightning sensor that

will provide continuous coverage over the North American sector, thereby providing a certain degree of redundancy in the lightning measurements in that sector.

In this paper we have shown some highlights from a seasonal and diurnal cycle lightning climatology constructed from WWLLN data binned hourly and in 0.25° × 0.25° grid boxes. The caveats raised by the analysis of Abarca et al. (2010) notwithstanding, the WWLLN lightning climatology appears to be consistent with in situ observations and with the TRMM rainfall climatology, and it provides a plausible representation of how the frequency of deep cumulus convection varies over the course of the day in the vicinity of coastlines and orography. Indeed, most of the features of the seasonal and diurnal cycles derived from WWLLN and the mechanisms that give rise to them have been known, or at leasted hinted at, for decades. What is new is the unprecedented ability to view the diurnal cycle in lightning from a global perspective with high spatial resolution. Although we have not illustrated it here, the large sample size of WWLLN data makes it possible to refine the analysis in order to investigate how the diurnal cycle in lightning changes with season and in response to day-to-day variations in wind patterns and vertical profiles of temperature and moisture. Such analyses will be useful for refining our understanding of the environmental conditions that give rise to intense convection and for validating numerical models that attempt to simulate the statistics of intense convection in a realistic setting.

Acknowledgments

The authors thank three anonymous reviewers for their helpful recommendations. This work was supported by the National Science Foundation under grant ATM 0812802 and by NOAA under contract NA10OAR4320148 AM62. Lightning location data were provided by

344 WWLLN (http://wwlln.net), a collaboration among over 50 universities and institutions. The
345 LIS/OTD climatologies were obtained from the NASA's Global Hydrology and Climate Center
346 (http://thunder.msfc.nasa.gov/). TRMM rainfall data were obtained from NASA's Goddard
347 Earth Sciences Data and Information Services Center (http://mirador.gsfc.nasa.gov/).
348
349 **References**

350 Abarca, S. F., K. L. Corbosiero, and T. J. Galarneau Jr., 2010: An evaluation of the Worldwide
351 Lightning Location Network (WWLLN) using the National Lightning Detection Network
352 (NLDN) as ground truth. *J. Geophys. Res.*, **115**, D18206, doi:10.1029/2009JD013411.
353 Altaratz, O., Z. Levin, Y. Yair, and B. Ziv, 2003: Lightning activity over land and sea on the
354 eastern coast of the Mediterranean. *Mon. Wea. Rev.*, **131**, 2060-2070.
355 Bendix, J., K. Trachte, J. Cermak, R. Rollenbeck, and T. Nauß, 2009: Formation of convective
356 clouds at the foothills of the tropical eastern Andes (South Ecuador). *J. Appl. Meteor.*
357 *Climatol.*, **48**, 1682-1695.
358 Boccippio, D. J., S. J. Goodman, and S. Heckman, 2000: Regional differences in tropical
359 lightning distributions. *J. Appl. Meteor.*, **39**, 2231-2248.
360 Boccippio, D. J., W. J. Koshak, and R. J. Blakeslee, 2002: Performance assessment of the
361 Optical Transient Detector and Lightning Imaging Sensor. Part I: Predicted diurnal
362 variability. *J. Atmos. Oceanic Technol.*, **19**, 1318-1332.
363 Christian, H. J., and Coauthors, 1999: The Lightning Imaging Sensor. *Proc. 11th Int. Conf. on*
364 *Atmospheric Electricity*, Guntersville, AL, International Commission on Atmospheric
365 Electricity, 726-729.

366 Christian, H. J., R. J. Blakeslee, S. J. Goodman, and D. M. Mach, 2000: Algorithm theoretical
367 basis document (ATBD) for the Lightning Imaging Sensor (LIS). [Available online at
368 http://gcmd.nasa.gov/records/01-algo2-99.html.]
369 Christian, H. J., and Coauthors, 2003: Global frequency and distribution of lightning as
370 observed from space by the Optical Transient Detector. *J. Geophys. Res.*, **108**, No. D1,
371 4005, doi:10.1029/2002JD002347.
372 Chronis, T. G., 2012: Preliminary lightning observations over Greece. *J. Geophys. Res.*, **117**,
373 D03113, doi:10.1029/2011JD017063.
374 Collier, A. B., A. R. W. Hughes, J. Lichtenberger, and P. Steinbach, 2006: Seasonal and diurnal
375 variation of lightning activity over southern Africa and correlation with European
376 whistler observations. *Ann. Geophys.*, **24**, 529-542.
377 Connaughton, V., and Coauthors, 2010: Associations between Fermi Gamma-ray Burst Monitor
378 terrestrial gamma ray flashes and sferics from the World Wide Lightning Location
379 Network. *J. Geophys. Res.*, **115**, A12307, doi:10.1029/2010JA015681.
380 Defer, E., K. Lagouvardos, and V. Kotroni, 2005: Lightning activity in the eastern
381 Mediterranean region. *J. Geophys. Res.*, **110**, D24210, doi:10.1029/2004JD005710.
382 Deierling, W., and W. A. Petersen, 2008: Total lightning activity as an indicator of updraft
383 characteristics. *J. Geophys. Res.*, **113**, D16210, doi:10.1029/2007JD009598.
384 Dowden, R. L., J. B. Brundell, and C. J. Rodger, 2002: VLF lightning location by time of group
385 arrival (TOGA) at multiple sites. *J. Atmos. Solar-Terr. Phys.*, **64**, 817-830.
386 Fujita, M., F. Kimura, and M. Yoshizaki, 2010: Morning precipitation peak over the Strait of
387 Malacca under a calm condition. *Mon. Wea. Rev.*, **138**, 1474-1486.

388 Gettelman, A., and P. M. de F. Forster, 2002: A climatology of the tropical tropopause layer. *J.*
389 *Metr. Soc. Japan*, **80**, 911-924.
390 Hamid, E. Y., Z.-I. Kawasaki, and R. Mardiana, 2001: Impact of the 1997-98 El Niño event on
391 lightning activity over Indonesia. *Geophys. Res. Lett.*, **28**, 147-150.
392 Highwood, E. J., and B. J. Hoskins, 1998: The tropical tropopause. *Quart. J. Roy. Meteor. Soc.*,
393 **124**, 1579-1604.
394 Hirose, M., R. Oki, S. Shimizu, M. Kachi, and T. Higashiuwatoko, 2008: Finescale diurnal
395 rainfall statistics refined from eight years of TRMM PR data. *J. Appl. Meteor. Climatol.*,
396 **47**, 544-561.
397 Hoskins, B. J., and K. I. Hodges, 2005: A new perspective on Southern Hemisphere storm
398 tracks. *J. Climate*, **18**, 4108-4129.
399 Hoskins, B. J., and P. J. Valdes, 1990: On the existence of storm tracks. *J. Atmos. Sci.*, **47**,
400 1854-1864.
401 Huffman, G. J., and Coauthors, 1997: The Global Precipitation Climatology Project (GPCP)
402 combined precipitation dataset. *Bull. Amer. Meteor. Soc.*, **78**, 5-20.
403 Huffman, G. J., and Coauthors, 2007: The TRMM Multisatellite Precipitation Analysis
404 (TMPA): Quasi-global, multiyear, combined-sensor precipitation estimates at fine scales.
405 *J. Hydrometeor.*, **8**, 38-18.
406 Hutchins, M. L., R. H. Holzworth, C. J. Rodger, and J. B. Brundell, 2012a: Far field power of
407 lightning strokes as measured by the World Wide Lightning Location Network. *J. Atmos.*
408 *Oceanic Technol.*, **29**, doi:10.1175/JTECH-D-11-00174.1.

409 Hutchins, M. L., R. H. Holzworth, J. B. Brundell, and C. J. Rodger, 2012b: Relative detection
410 efficiency of the World Wide Lightning Location Network. *Radio Sci.*, 2012RS005049
411 (submitted).
412 Jackson, B., S. E. Nicholson, and D. Klotter, 2009: Mesoscale convective systems over western
413 equatorial Africa and their relationship to large-scale circulation. *Mon. Wea. Rev.*, **137**,
414 1272-1294.
415 Jacobson, A. R., R. Holzworth, J. Harlin, R. Dowden, and E. Lay, 2006: Performance
416 assessment of the World Wide Lightning Location Network (WWLLN) using the Los
417 Alamos Sferic Array (LASA) as ground truth. *J. Atmos. Oceanic Technol.*, **23**, 1082,
418 doi:10.1175/JTECH1902.1.
419 Jansa, A., A. Genoves, M. Angeles Picornell, J. Campins, R. Riosalido, and O. Carrettero, 2001:
420 Western Mediterranean cyclones and heavy rain. Part 2: Statistical approach.
421 *Meteorological Applications*, **8**, 43-56.
422 Johnson, R. H., T. M. Rickenbach, S. A. Rutledge, P. E. Ciesielski, and W. H. Schubert, 1999:
423 Trimodal characteristics of tropical convection. *J. Climate*, **12**, 2397-2418.
424 Kandalgaonkar, S. S., M. I. R. Tinmaker, J. R. Kulkarni, and A. Nath, 2003: Diurnal variation of
425 lightning activity over the Indian region. *Geophys. Res. Lett.*, **30**, No. 20,
426 doi:10.1029/2003GL018005.
427 Karas, S., and A. Zangvil, 1999: A preliminary analysis of disturbance tracks over the
428 Mediterranean basin. *Theor. Appl. Climatol.*, **64**, 239-248.
429 Katsanos, D., K. Lagouvardos, V. Kotroni, and A. Argiriou, 2007: Combined analysis of rainfall
430 and lightning data produced by mesoscale systems in the central and eastern
431 Mediterranean. *Atmospheric Research*, **83**, 55-63.

Kikuchi, K., and B. Wang, 2008: Diurnal precipitation regimes in the global tropics. *J. Climate*, **21**, 2680-2696.

Kodama, Y.-M., M. Tokuda, and F. Murata, 2006: Convective activity over the Indonesian Maritime Continent during CPEA-I as evaluated by lightning activity and Q1 and Q2 profiles. *J. Meteor. Soc. Japan.*, **84A**, 133-149.

Kotroni, V., and K. Lagouvardos, 2008: Lightning occurrence in relation with elevation, terrain slope, and vegetation cover in the Mediterranean. *J. Geophys. Res.*, **113**, D21118, doi:10.1029/2008JD010605.

Liu, C., and E. J. Zipser, 2008: Diurnal cycles of precipitation, clouds, and lightning in the tropics from 9 years of TRMM observations. *Geophys. Res. Lett.*, **35**, L04819, doi:10.1029/2007GL032437.

Lopez, R. E., 1978: Internal structure and development processes of C-scale aggregates of cumulus clouds. *Mon. Wea. Rev.*, **106**, 1488-1494.

Mahrer, Y., and R. A. Pielke, 1977: The effects of topography on sea and land breezes in a two-dimensional numerical model. *Mon. Wea. Rev.*, **105**, 1151-1162.

Mapes, B. E., T. T. Warner, and M. Xu, 2003: Diurnal patterns of rainfall in northwestern South America. Part III: Diurnal gravity waves and nocturnal convection offshore. *Mon. Wea. Rev.*, **131**, 830-844.

Mori, S., and Coauthors, 2004: Diurnal land-sea rainfall peak migration over Sumatera Island, Indonesian Maritime Continent, observed by TRMM satellite and intensive rawinsonde soundings. *Mon. Wea. Rev.*, **132**, 2021-2039.

Ogura, Y., and T. Takahashi, 1971: Numerical simulation of the life cycle of a thunderstorm cell. *Mon. Wea. Rev.*, **99**, 895-911.

455 Orville, R. E., and D. W. Spencer, 1979: Global lightning flash frequency. *Mon. Wea. Rev.*,
456 **107**, 934-943.
457 Pessi, A. T., and S. Businger, 2009: Relationships among lightning, precipitation, and
458 hydrometeor characteristics over the North Pacific Ocean. *J. Appl. Meteor. Climatol.*, **48**,
459 833-848.
460 Petersen, W. A., S. A. Rutledge, and R. E. Orville, 1996: Cloud-to-ground lightning
461 observations from TOGA COARE: Selected results and lightning location algorithms.
462 *Mon. Wea. Rev.*, **124**, 602-620.
463 Pinto, I. R. C. A., O. Pinto Jr., R. M. L. Rocha, J. H. Diniz, A. M. Carvalho, and A. Cazetta
464 Filho, 1999: Cloud-to-ground lightning in southeastern Brazil in 1993. *J. Geophys. Res.*,
465 **104**, 31381-31387.
466 Qian, J.-H., 2008: Why precipitation is mostly concentrated over islands in the Maritime
467 Continent. *J. Atmos. Sci.*, **65**, 1428-1441.
468 Rickenbach, T. M., and S. A. Rutledge, 1998: Convection in TOGA COARE: Horizontal scale,
469 morphology, and rainfall production. *J. Atmos. Sci.*, **55**, 2715-2729.
470 Rodger, C. J., J. B. Brundell, R. L. Dowden, and N. R. Thomson, 2004: Location accuracy of
471 long distance VLF lightning location network. *Ann. Geophys.*, **22**, 747-758.
472 Rodger, C. J., J. B. Brundell, and R. L. Dowden, 2005: Location accuracy of VLF World-Wide
473 Lightning Location (WWLL) network: Post-algorithm upgrade. *Ann. Geophys.*, **23**, 277-
474 290.
475 Rodger, C. J., S. Werner, J. B. Brundell, E. H. Lay, N. R. Thomson, R. H. Holzworth, and R. L.
476 Dowden, 2006: Detection efficiency of the VLF World-Wide Lightning Location
477 Network (WWLLN): Initial case study. *Ann. Geophys.*, **24**, 3197-3214.

478 Rodger, C. J., J. B. Brundell, R. H. Holzworth, E. H. Lay, N. B. Crosby, T.-Y. Huang, and M. J.
479 Rycroft, 2009: Growing detection efficiency of the World Wide Lightning Location
480 Network. *AIP Conference Proceedings*, 15-20, doi:10.1063/1.3137706.
481 Rudlosky, S. D., and H. E. Fuelberg, 2010: Pre- and postupgrade distributions of NLDN
482 reported cloud-to-ground lightning characteristics in the contiguous United States. *Mon.*
483 *Wea. Rev.*, **138**, 3623-3633.
484 Salio, P., M. Nicolini, and E. J. Zipser, 2007: Mesoscale convective systems over southeastern
485 South America and their relationship with the South American low-level jet. *Mon. Wea.*
486 *Rev.*, **135**, 1290-1309.
487 Savijärvi, H., and S. Järvenoja, 2000: Aspects of the fine-scale climatology over Lake
488 Tanganyika as resolved by a mesoscale model. *Meteor. Atmos. Phys.*, **73**, 77-88.
489 Schultz, D. M., and C. A. Doswell, 2000: Analyzing and forecasting Rocky Mountain lee
490 cyclogenesis often associated with strong winds. *Wea. Forecasting*, **15**, 152-173.
491 Schumacher, C., and R. A. Houze Jr., 2003: Stratiform rain in the tropics as seen by the TRMM
492 precipitation radar. *J. Climate*, **16**, 1739-1756.
493 Stith, J. L., J. E. Dye, A. Bansemer, A. J. Heymsfield, C. A. Grainger, W. A. Peterson, and R.
494 Cifelli, 2002: Microphysical observations of tropical clouds. *J. Appl. Meteor.*, **41**, 97-
495 117.
496 Tapia, A., J. A. Smith, and M. Dixon, 1998: Estimation of convective rainfall from lightning
497 observations. *J. Appl. Meteor.*, **37**, 1497-1509.
498 Turman, B. N., 1978: Analysis of lightning data from the DMSP satellite. *J. Geophys. Res.*, **83**,
499 5019-5024.

Williams, E., and N. Renno, 1993: An analysis of the conditional instability of the tropical atmosphere. *Mon. Wea. Rev.*, **121**, 21-36.

Wu, P., M. Hara, J.-I. Hamada, M. D. Yamanaka, and F. Kimura, 2009: Why a large amount of rain falls over the sea in the vicinity of western Sumatra Island during nighttime. *J. Appl. Meteor. Climatol.*, **48**, 1345-1361.

Yuan, J., R. A. Houze, and A. J. Heymsfield, 2011: Vertical structures of anvil clouds of tropical mesoscale convective systems observed by CloudSat. *J. Atmos. Sci.*, **68**, 1653-1674.

Zishka, K. M., and P. J. Smith, 1980: The climatology of cyclones and anticyclones over North America and surrounding ocean environs for January and July, 1950-77. *Mon. Wea. Rev.*, **108**, 387-401.

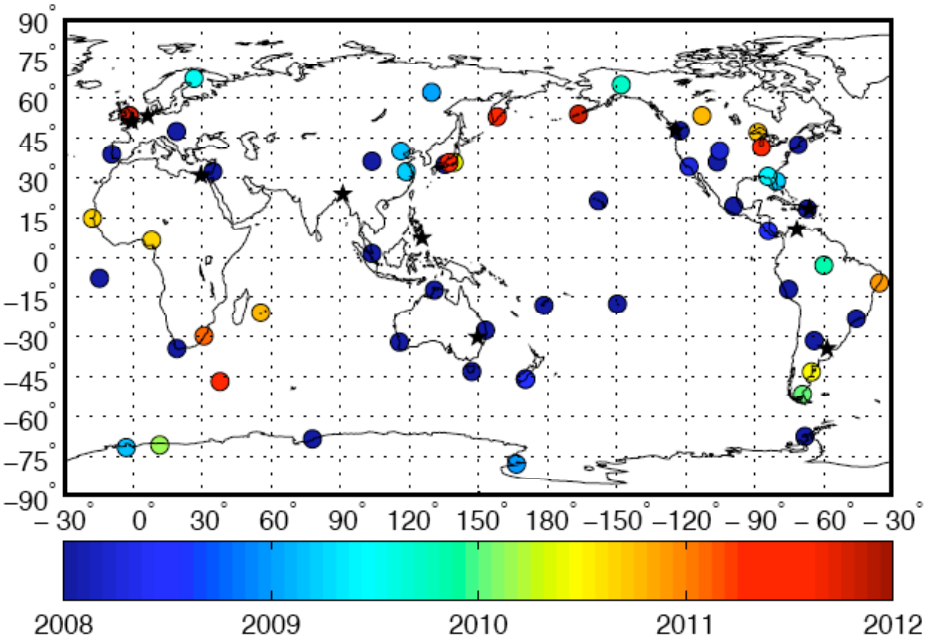

510 Figure 1. Location of WWLLN sensors, color-coded according to the date each was established.
511 Stations established prior to 2008 are shown in dark blue; black stars indicate stations established
512 2012-present.
513

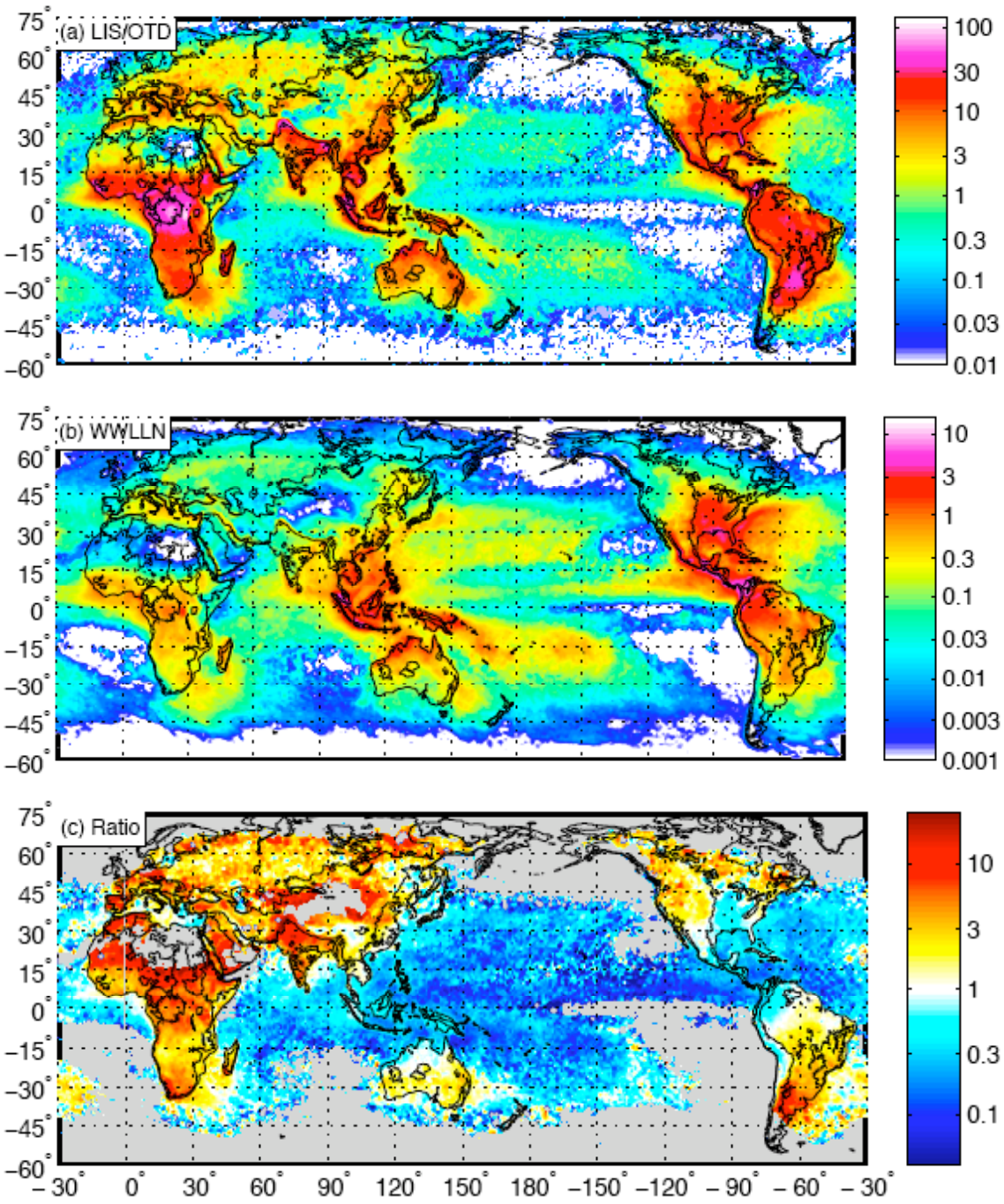

513 Figure 2. Annual-mean frequency of occurrence of lightning from LIS/OTD (*a*; flashes km^{-2}
514 yr^{-1}) and WWLLN (*b*; strokes km^{-2} yr^{-1}). Ratio of LIS/OTD to WWLLN strokes, scaled by the
515 mean of each dataset (*c*; gray shading indicates either no LIS/OTD lightning flashes or WWLLN
516 lightning frequency < 0.01 strokes km^{-2} yr^{-1}; see text for details). All fields have been averaged
517 on a 1° × 1° grid. Black contours indicate the 500-m elevation.

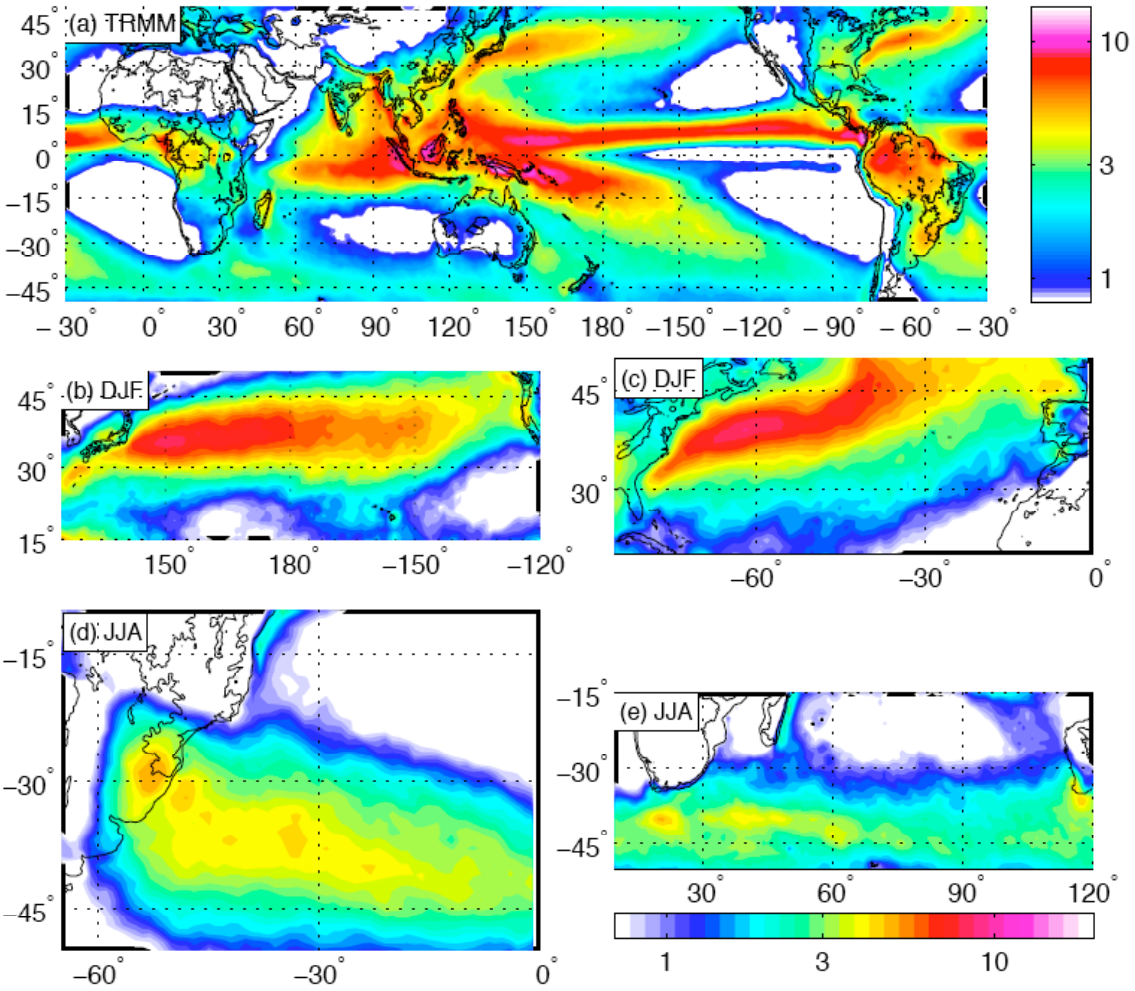

518 Figure 3. TRMM annual-mean (*a*) and seasonal-mean precipitation (*b* to *e*; mm day^{-1}; 1° × 1°
519 resolution). Black contours indicate the 500-m elevation.

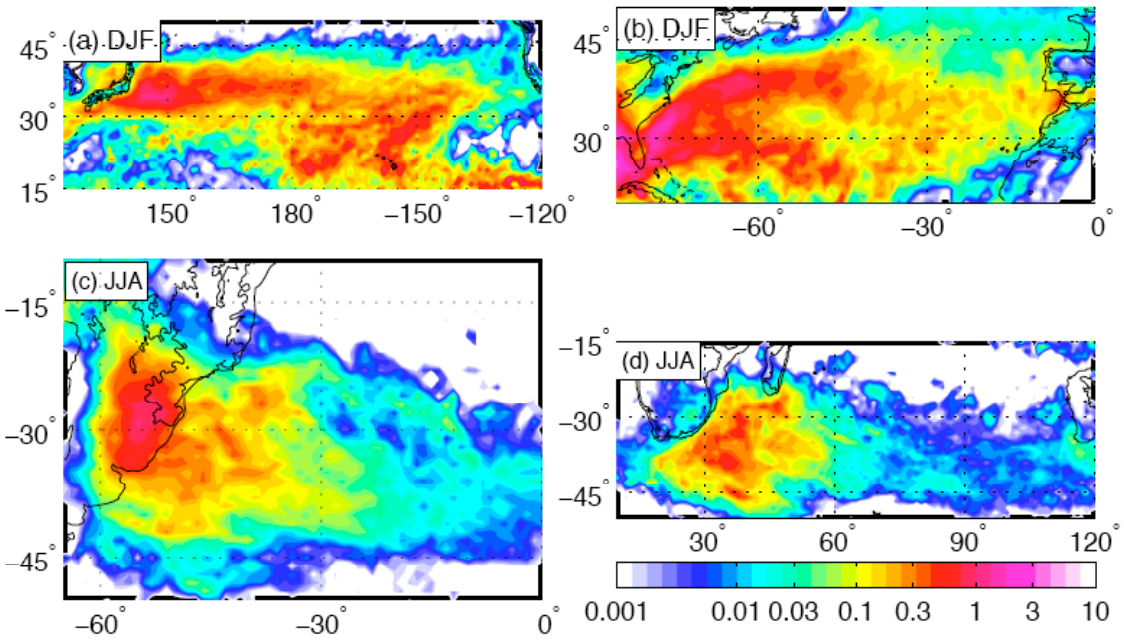

520 Figure 4. WWLLN seasonal-mean lightning frequency (strokes km^{-2} yr^{-1}; 1° × 1° resolution)
521 during December-February (DJF; *a*, *b*) and June-August (JJA; *c*, *d*). Black contours indicate the
522 500-m elevation.
523

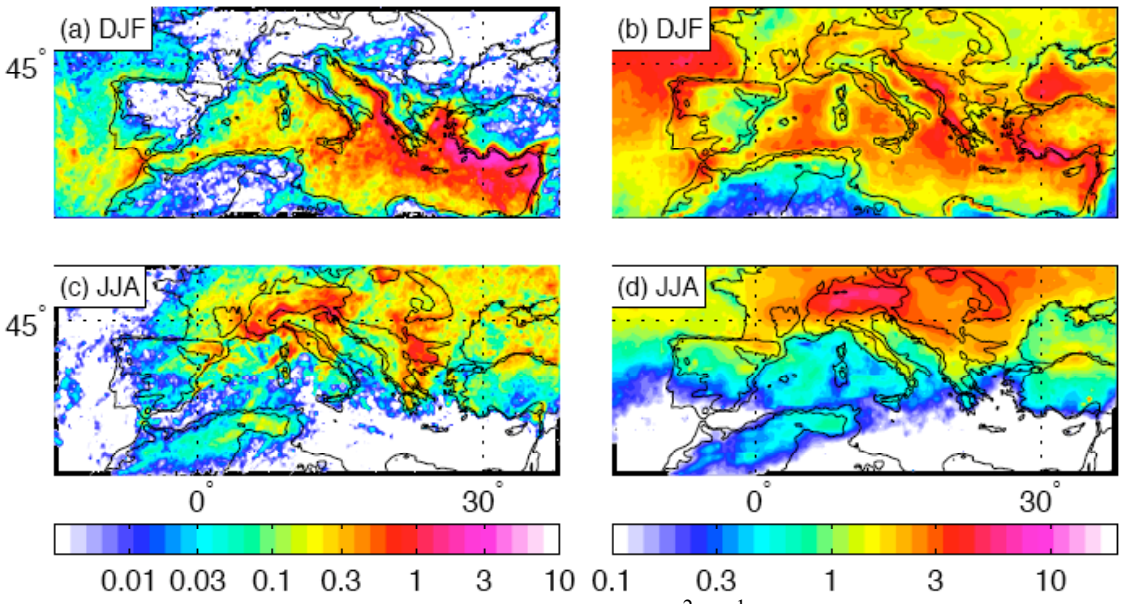

523 Figure 5. WWLLN lightning frequency (*a*, *c*; strokes km^{-2} yr^{-1}) and TRMM 3B42 precipitation
524 (*b*, *d*; mm day^{-1}; both at 0.25° × 0.25° resolution) during DJF (*a*, *b*) and JJA (*c*, *d*). Black
525 contours indicate the 500-m elevation.

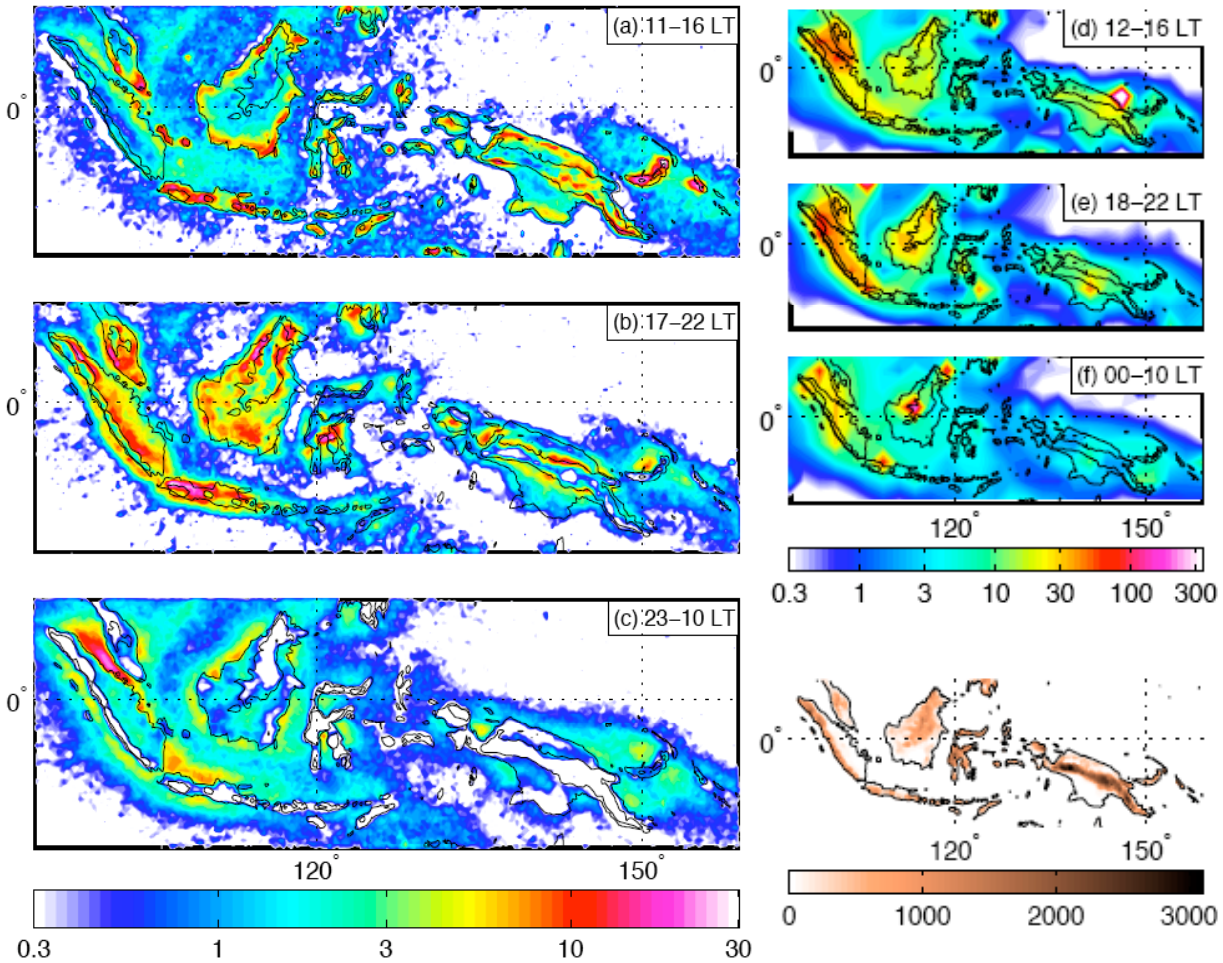

526 Figure 6. WWLLN lightning frequency (*a-c*; strokes km^{-2} yr^{-1}; hourly, 0.25° × 0.25° resolution)
527 and LIS/OTD lightning frequency (*d-f*; flashes km^{-2} yr^{-1}; two-hourly, 2.5° × 2.5° resolution) for
528 indicated time intervals during all months. Local time given for Singapore. Black contours
529 indicate the 500-m elevation. Elevation (m) in (*g*).
530
531

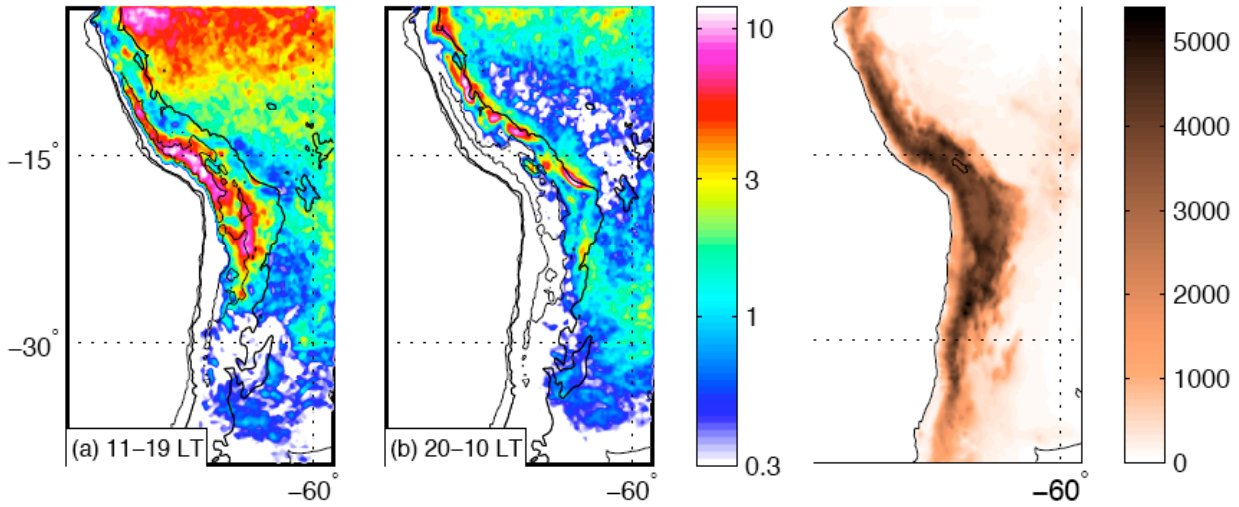

531 Figure 7. WWLLN lightning frequency (strokes km^{-2} yr^{-1}; 0.25° × 0.25° resolution) over the
532 central Andes for indicated time intervals during November-March. Local time given for Lima,
533 Peru. Black contours indicate the 500-m and 4000-m elevation. Elevation (m) in (*c*).
534

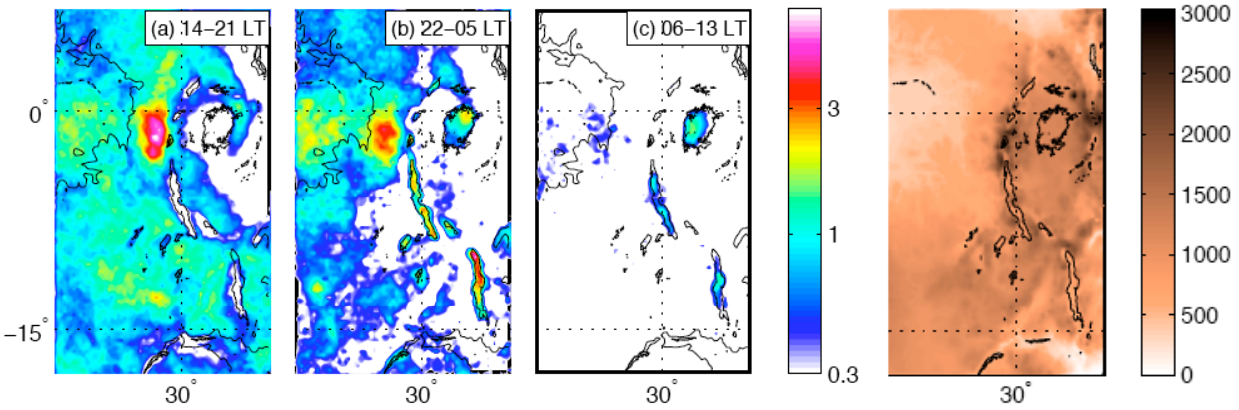

534 Figure 8. As in Fig. 7, but for tropical Africa for all months. Local time given for Kampala,
535 Uganda.
536